Field-Frequency Locked In Vivo Proton MRS on a Whole-Body Spectrometer

Pierre-Gilles Henry,[1] Pierre-François van de Moortele,[1] Eric Giacomini,[1] Arno Nauerth,[2] and Gilles Bloch,[1]*

The stability of the main magnetic field is critical for prolonged in vivo magnetic resonance spectroscopy (MRS) acquisitions, especially for difference spectroscopy. This study was focused on the implementation and optimization of a field-frequency lock (FFL) on a whole body spectrometer, to correct the main field drift during localized proton MRS of the human brain. The FFL was achieved through a negative feed-back applied in real time on the Z0 shim coil current, after calculation of the frequency shift from a reference signal. This signal was obtained from the whole head with a small flip angle acquisition interleaved with the PRESS acquisition of interest. To avoid propagation of the important short-term time-correlated fluctuations of the head water frequency (mainly due to respiratory motion) onto Z0 correction, the sampling rate of the reference frequency and the smoothing window for the Z0 correction were carefully optimized. Thus, an effective FFL was demonstrated in vivo with no significant increase of the short-term variance of the water frequency. Magn Reson Med 1999 42:636–642, 1999. © 1999 Wiley-Liss, Inc.

The main field stability of NMR superconducting magnets normally ensures a very slow frequency drift, generally below 0.1 ppm/hr. Over the last few years the spectral resolution of in vivo proton MRS has been greatly improved by the combined use of high-field magnets and efficient computer assisted shimming procedures, including the adjustment of second-order shims (1). Singlet linewidths as low as 0.015 ppm were obtained in the dog brain at 9.4 T. Even at field strengths of 2–4 T, where singlet linewidths below 0.05 ppm are currently achieved in the human brain, spectrometer frequency must be adjusted several times per hour during prolonged proton MRS studies, in order to maintain an optimal water suppression (2,3) or a stable efficiency of highly selective editing pulses (4,5) and to avoid line broadening when extensive data accumulation is necessary. Most often, the frequency update is performed between two successive spectra by measuring the water frequency on a single scan. This interruption of data accumulation always represents a waste of time and may be difficult to manage during chemical-shift imaging (CSI) or two-dimensional (2D) experiments, which can last several tens of minutes. An increased stability of the main magnetic field would also significantly improve the robustness of spectroscopic measurements based on difference spectra, where strong subtraction artifacts are induced by minute frequency shifts.

Spectrometer frequency update becomes critical in situations of rapid main field drift (above the limit of 0.1 ppm/hr, usually specified by manufacturers), which can be related to an external perturbation in an hostile environment, to a defect in the superconducting coil, or to temperature variation in the passive iron shims of the magnet. The last case, which was the initial motivation of the present study, is encountered for magnet designs where the resistive active shim coils are thermally coupled to the passive iron shims, when high shim currents are applied. This unfavorable situation is rather specific to high-field systems, because high currents are required in second-order shim coils to achieve the above-mentioned gain in spectral resolution. The resulting field drift can reach several-fold the value specified by magnet manufacturers (a specification generally controlled with all shim currents to zero) so that field drift compensation appears mandatory. While field-frequency lock through a deuterium channel is ubiquitous in high-resolution NMR to ensure long-term stability of spectrometer frequency, large bore horizontal systems used for in vivo MRS do not comprise the hardware required to offer this possibility. In addition, many practical difficulties, such as the positioning of the deuterium probe and sample or the interference of the use of the gradients with the reference deuterium signal, disqualify this classical solution for localized in vivo MRS.

In this study, we demonstrate that field-frequency lock can be achieved during localized proton MRS of the human brain, by interleaving the acquisition of interest with a small flip angle acquisition to monitor the non-localized whole head water as a reference signal. This alternative approach exploits the possibility offered by modern spectrometers to process acquired data on the fly and does not require significant modifications of the spectrometer hardware.

MATERIALS AND METHODS

The field-frequency lock was implemented on a BRUKER (Wissembourg, France) AVANCE spectrometer interfaced to an OXFORD (Oxford, United Kingdom) whole-body 3 T magnet. The principle of the method is depicted in Figure 1 and is based on correcting the field by a negative feed-back applied on the Z0 shim coil current, after calculation of the frequency shift from a reference signal. The reference water
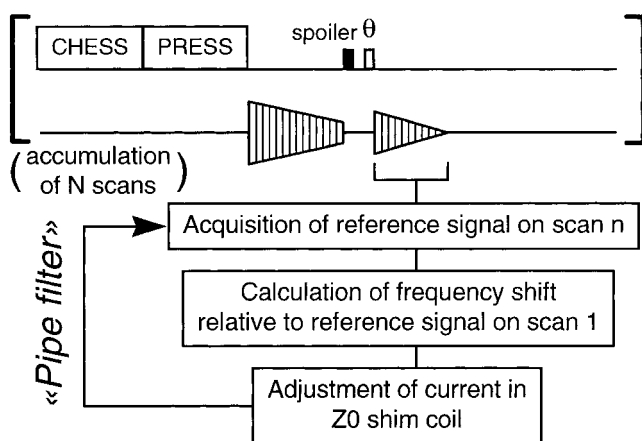
FIG. 1. Flowchart of the field-frequency lock.

signal was collected (512 complex points, 0.5 msec sampling interval) through a non-localized pulse-acquire acquisition added at the end of a PRESS sequence (6).

During data accumulation, each PRESS scan was interleaved with a reference scan and a spoiler gradient was applied after each PRESS acquisition to eliminate any residual transverse magnetization. Using the « pipe filter » capability of BRUKER ParaVision software, each reference scan was processed in real time on the spectrometer workstation (INDY, Silicon Graphics) to calculate the frequency shift of the water signal, and the result was used to update the current delivered in the Z0 shim coil. The frequency shift was determined by comparing the reference signal acquired at the end of the nth scan to that acquired at the end of the first scan of the currently accumulating spectrum. It is well known that a frequency shift $\Delta \nu$ corresponds to a linear phase shift of $2\pi\Delta\nu t$ during the acquisition time t. Thus, the phase difference $\Delta\varphi(t) = 2\pi\Delta\nu t$ between the two reference FIDs was computed for each complex point in time t, and the linear phase shift was estimated using a non-iterative least-squares fit of $\Delta\varphi(t)$ versus t. The slope of this fit, expressed in turns per second, directly gives the frequency shift $\Delta\nu$ between the two reference scans. To reduce the influence of too noisy data, the modulus of each time point in the first scan was introduced as a weighting function of the fit. In addition, the average modulus of the last 200 points of the first scan was calculated and the time points exhibiting a modulus below five times this value were not taken into account in the fit. As a consequence of this threshold, only 100–200 time points were effectively used.

With this approach, the time required to perform the frequency shift and Z0 correction calculations was about 50 msec. However, the time necessary for the Z0 shim update was much longer, about 800 msec, to address the command from the spectrometer workstation to the shim power supply, and 400 msec for the stabilization of the shim current at the new value. Thus, with the present hardware, the minimum TR of the sequence depicted in Fig. 1 was limited to about 2 sec. To reduce the minimum available increment in the Z0 shim current adjustment, a current divider was installed on the Z0 channel at the output of the shim power supply. This was the only

hardware modification required to implement the field-frequency lock.

Due to respiratory and cardiac motion, the frequency of the non-localized head water signal fluctuates on a short time scale, in addition to the long-term field drift (see Results). Because these fluctuations are time correlated, the sampling rate of the reference frequency and the smoothing for the Z0 adjustment must be carefully optimized. This was first achieved by using numerical simulations programmed with MatLab (The MathWorks). Then, the findings from the simulations and the effectiveness of the field-frequency lock were tested on the spectrometer by performing experiments on a water phantom. For these studies, a controlled variation of the water frequency was applied independently from the Z0 shim currents by using minute variations of the Z2 shim current, which did not significantly affect the water line shape.

The field-frequency lock was finally validated in vivo. Proton MRS of the brain was performed on one of the co-authors using a BRUKER quadrature bird-cage coil. The head of the subject was strapped to the head holder in order to restrain potential motion. The interleaved PRESS/pulse-acquire sequence was run in an occipital voxel of 15 ml, with a TE of 68 msec and a TR of 2 or 3 sec. A rapid main field drift (up to 0.5 ppm/hr or 1 Hz/min, and expressed thereafter in proton frequency unit) was observed due to heating of the passive shims of the magnet when intense second-order shim currents were applied. A similar drift, also due to passive shims heating, was induced for demonstration purpose by running the gradients with a heavy duty cycle and without water cooling for a few minutes. The effect of the field drift on the spectral lines was assessed by measuring manually, with the ParaVision software, the full width at half-height of the N-acetyl aspartate resonance at 2.0 ppm.

RESULTS

In spite of a broad linewidth and a shorter acquisition time for the reference signal (256 msec), the global frequency shift of the water proton spectrum can be monitored with a high accuracy, as illustrated in Figure 2. A series of reference signals were acquired with the interleaved PRESS/pulse-acquire sequence on a water phantom shimmed to a water linewidth representative of the in vivo situation (about 90 Hz). The water signal frequency variation was estimated from the non-localized data using three different methods. Method A is the time-domain fitting described in Materials and Methods. In method B, each reference FID was Fourier-transformed, after zero-filling to 128K complex points, and the frequency of the maximum amplitude was determined on the magnitude spectrum. In method C, a correlation analysis was used to calculate the frequency shift between two magnitude spectra (reference scan n vs. reference scan 1) obtained after zero-filling to 128 K complex points and FFT. The excellent agreement between these three methods (Fig. 2) indicates that the frequency shift due to the magnet field drift can be monitored with a resolution below 0.1 Hz, even on a broad water signal. On the other hand, the time required to compute a frequency shift with method C on the spectrometer workstation, about 30 sec, is not compatible with the TRs generally used
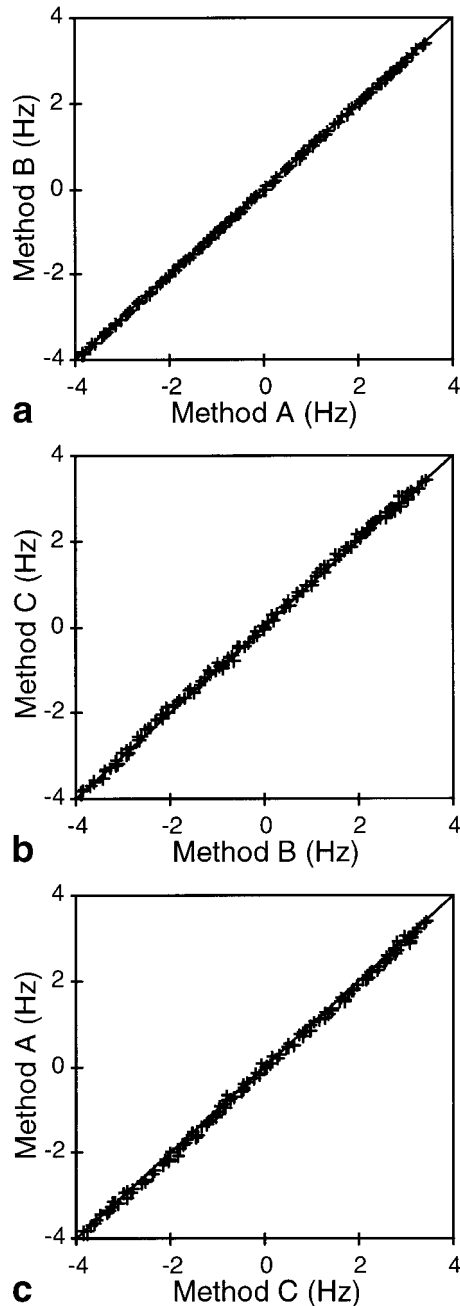
FIG. 2. **a–c:** Comparison between three measurement methods to determine the frequency variation from a broad proton signal (linewidth of about 90 Hz) obtained on a water phantom through the small flip angle pulse-acquire segment of the interleaved sequence shown in Fig. 1. The field drift was induced by varying the Z0 shim current and 128 measurements were performed. The experimental points are plotted as crosses and the continuous line represents identity.

for in vivo MRS. Method A was retained for the field-frequency lock, first because it is much faster than method B: 50 msec vs. 2 sec for a frequency shift calculation. In addition, the time-domain fitting appeared more robust than the peak peaking toward small deformations of the in vivo whole head water signal. These minor perturbations can indeed affect the position of the maximal amplitude of the spectrum estimated by method B, but do not significantly interfere with the global shift of the spectrum estimated by method A.

As illustrated in Figure 3, the variation of the head water signal frequency over time can be attributed to three main components: the long-term frequency drift, which we want to compensate for and which was mainly due in this case to passive iron shims heating through intense currents in the active shims; the respiration of the subject, which induces a pseudo-periodic oscillation of the frequency; and additional noise, related to cardiac cycle and other rapid small movements. In this particular example, where the subject's breathing was paced at $1/3.5$ Hz by an auditory cue, while the MRS sequence was run with a TR of 3 sec, the truly periodic fluctuation related to respiration clearly dominates the short-term variance of the water frequency. This was confirmed quantitatively by removing the long-term drift, through a linear fit, from the frequency plots shown in Fig. 3a and c: the variance of these processed data drops from 0.143 to 0.045 Hz^2 when the strong peak corresponding to respiration in the Fourier transform of the water frequency time course is replaced by the mean of its neighboring points (Fig. 3b,d).

In order to avoid propagation of the water signal frequency short-term fluctuations onto Z0 correction, optimum parameters must be determined for calculating this correction from previous water signal frequency measurements. Unlike non-correlated noise, whose influence can be simply minimized by averaging several successive frequency measurements to determine the Z0 shim correction, time-correlated frequency fluctuations can dramatically increase the short-term variance, if an inappropriate smoothing window is applied. The simulations in Figure 4 illustrate this feature: the spontaneous variation of the water signal frequency, due to breathing, was modeled as a pure sinusoidal function $F_{resp}(t) = A.\sin(\nu_R \cdot t)$ where t is the time, ν_R is the respiration rate, and A is an arbitrary amplitude factor. For given values of TR and of the number of reference frequency measurements to be averaged (NA), the field-frequency lock was simulated numerically. For each value of ν_R, the effective frequency $F_{eff}(t)$ was calculated as the sum of $F_{resp}(t)$ and $F_{corr}(t)$, the frequency correction applied by the field-frequency lock. The plots in Fig. 4 represent the ratio $\sigma^2(F_{eff})/\sigma^2(F_{resp})$, where σ^2 denotes the time variance of the function. In the first example (Fig. 4a), it is clear that the field-frequency lock can increase the variance of the frequency for values of ν_R that are within the respiratory physiological range. On the other hand, with the more judicious choice of TR 2 sec and NA 6 (Fig. 4b), the field-frequency lock does not alter significantly the short-term variance of the frequency for any value of ν_R within the physiological range.

The agreement between these numerical simulations and the practical implementation of the field-frequency lock on the NMR spectrometer was tested on a water phantom. The « worst case » corresponding to the arrow in Fig. 4a (TR 3 sec, NA 4, oscillation rate 0.29 Hz) was achieved experimentally by running the field-frequency lock while the spontaneous water frequency was varied sinusoidally through the Z2 shim. As shown in Figure 5a, the effective water frequency time course (bottom trace), resulting from the addition of the spontaneous frequency (top trace) and of the field-frequency lock Z0 correction (middle trace), exhibited a variance exactly two times higher than the variance of the spontaneous frequency.

FIG. 3. Time-course (**a**) and Fourier analysis (**b**) of the whole head water frequency monitored with a TR of 3 sec on a subject breathing with a period of 3.5 sec. The strong peak at 0.05 Hz in **b** corresponds to the respiratory frequency (0.29 Hz) folded into the bandwidth effectively sampled (0–0.17 Hz). The low-frequency component is due to the long-term drift, which was approximated to a linear term in the time domain (dotted line in **a** and **c**). The contribution from the respiration to the short-term variance of the time-domain data can be estimated by canceling the respiratory peak in the Fourier transform (replaced by the mean of the neighboring points) (**d**) and by applying an inverse Fourier transform (**c**).
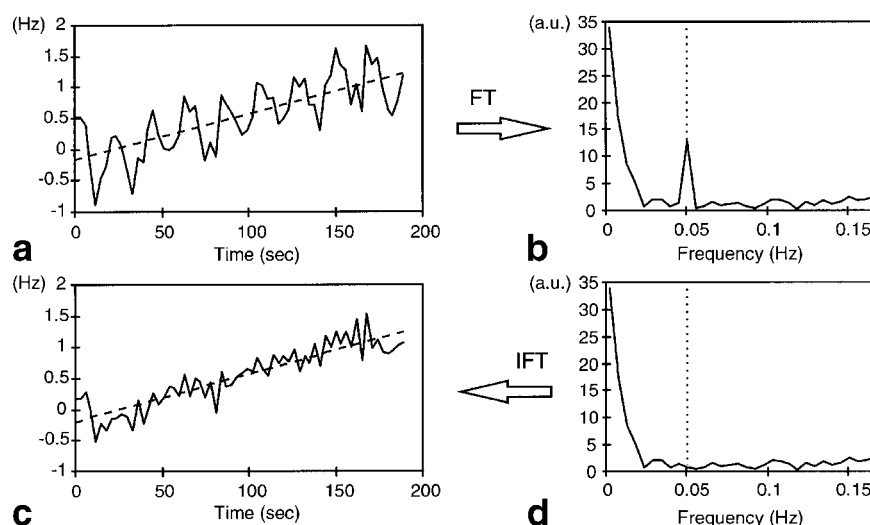
This pejorative effect is simply explained by the additive contribution from the Z0 correction oscillation, which is almost perfectly in phase with the spontaneous frequency oscillation. A similar effect was evidenced for data recorded in vivo (Fig. 5b) when the subject's breathing was paced by an auditory cue. The degradation of the short-term variance of the whole head water signal frequency by the field-frequency lock appeared less critical on a subject

FIG. 4. Numerical simulations of the effect of the field-frequency lock on the variance of the water signal frequency. The time course of the frequency was modeled as a pure sinusoidal function, mimicking the respiratory oscillation at a rate ν_R. **a, b:** Calculated ratio of the variance obtained with and without lock as a function of ν_R for (**a**) TR 3 sec, NA 4, and (**b**) TR 2 sec, NA 6. The dotted area corresponds to the respiratory physiological range. The arrow in **a** indicates the « worst case » used for the experiments shown in Fig. 5.

breathing normally (without use of an auditory cue). This results first from fluctuations of the respiratory rate, which cause some smoothing of the simulated plots in Fig. 4. Second, as shown in Fig. 3, additional sources of variance can reduce the relative importance of respiration.

However, to make the field-frequency lock as robust as possible in any situation, the parameters TR 2 sec and NA 6 were kept for the in vivo applications. Figure 6 shows a set of data obtained on one of the co-authors breathing normally (without use of an auditory cue), while the field of the magnet was drifting at about 1 Hz/min due to the heating of the passive iron shims. The plots in Fig. 6a clearly demonstrate that the long-term frequency drift was compensated by the field-frequency lock. On the other hand, the short-term variance of the reference signal frequency was only marginally altered: by subtracting, through a fourth order polynomial fit, the long-term drift from the spontaneous frequency variation, one can estimate that the short-term variance increased only from 0.054 to 0.057 Hz^2. Finally, because of the significant magnitude of the magnet field drift (about 1 Hz/min) on the time scale of the spectrum accumulation (total accumulation time of 8.5 min), the field-frequency lock resulted in a clear improvement in the linewidth of the metabolite spectra recorded in the occipital lobe of the brain with the PRESS sequence (Fig. 6b,c). Thus, the linewidth of the N-acetyl aspartate singlet was reduced by 2.5 Hz, leading to a full width at half-height of 6.6 Hz before lorentzian filtering.

DISCUSSION

This study demonstrates that an effective field-frequency lock can be implemented for brain localized proton MRS on a whole body spectrometer, without significant hardware modification. The proposed method uses a single coil for acquiring, in an interleaved mode, the localized spectroscopic data of interest and a reference water signal obtained from the whole head with a small flip angle. The frequency drift estimated from the reference signal is used to calculate and to apply in real-time a field correction through the Z0 shim. The experimental validation of the method was performed with a PRESS sequence and a volume coil, but the same approach could be directly used

a

b
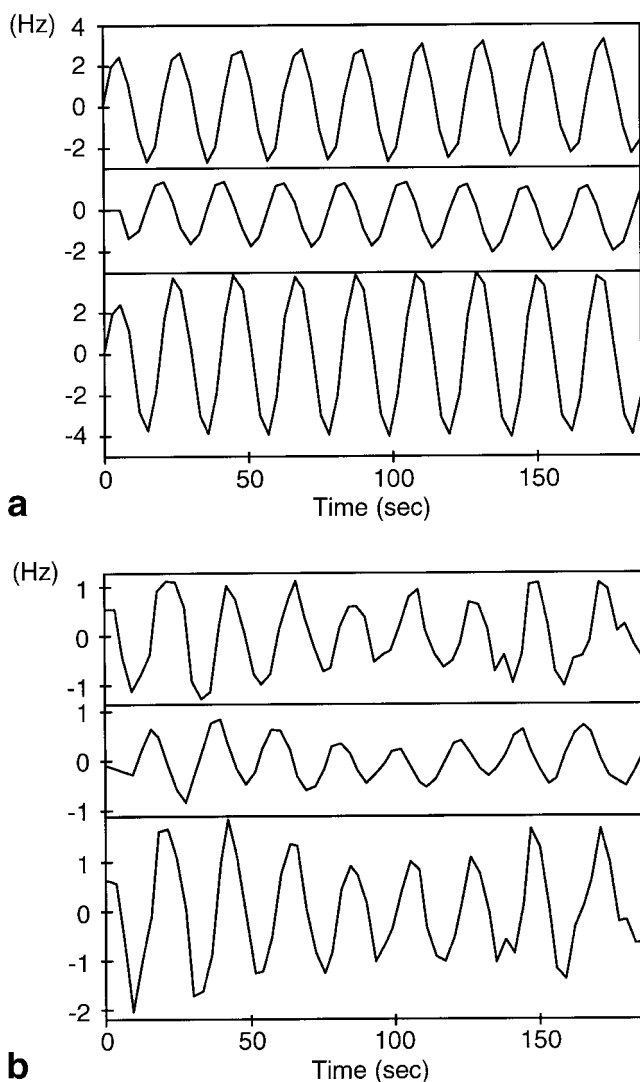
FIG. 5. In vitro and in vivo experimental demonstration of the effect of the field-frequency lock on the variance of the water frequency time course. **a:** Using a water phantom, the spontaneous frequency (top trace) was varied sinusoidally through the Z2 shim, while the field-frequency lock was run to adjust the Z0 correction (middle trace) with the parameters corresponding to Fig. 4a (TR 3 sec, NA 4, oscillation rate 0.29 Hz). The resultant frequency fluctuation (bottom trace) exhibited a variance increased by a factor of 2 compared with the spontaneous fluctuation, as predicted from the simulation in Fig. 4a. **b:** The time-course of the whole head water frequency was monitored on a subject breathing with a period of 3.5 sec, while the field-frequency lock was run to adjust the Z0 correction (middle trace) with the parameters corresponding to Fig. 4a (TR 3 sec, NA 4). The resultant frequency fluctuation (bottom trace) exhibited a variance significantly increased compared with the spontaneous fluctuation (top trace): 0.96 Hz^2 vs 0.49 Hz^2.

for any spectroscopic technique providing a long enough TR to apply the Z0 correction, and with other coil geometries. In addition, for experiments requiring a shorter TR, like CSI, variants of the proposed method could be easily designed, for example by updating the Z0 shim at intervals longer than the TR.

The reliability of the field-frequency lock depends on the accuracy of the reference frequency determination. Even if measuring a reference frequency directly from the local-

ized scan of interest (the PRESS acquisition in our case), on the residual water peak or on a metabolite resonance exhibiting a high enough signal-to-noise ratio (SNR), seems feasible and would have simplified the pulse sequence, a separate acquisition of the reference signal was preferred because of its more general applicability. In many cases, where the scan of interest exhibits a low SNR (small voxel) or a high intrinsic instability (ISIS localization, CSI), using a separate reference scan is indeed less problematic. Through a small flip angle pulse-acquire acquisition, a strong and stable reference water signal was obtained with less than 1% loss of the longitudinal magnetization available for the next PRESS acquisition. Moreover, we have shown that the broad line shape of the non-localized water signal is not a real limitation to the accuracy of the frequency drift monitoring.

A more difficult issue is the important short-term fluctuation of the head water signal frequency, mainly due to respiratory motion. This phenomenon is especially obvious in brain spectroscopy at high field. At 3 T, pseudo-periodic oscillations with an amplitude of 1–2 Hz peak to peak are generally observed. These frequency oscillations were not affected by restraining subject head motion, so that their most likely explanation is a direct perturbation of the whole head static field through the motion of the diaphragm, which appears as a large interface between air and dense tissues. One could think about minimizing these oscillations by adjusting the Z0 correction prospectively. The instantaneous frequency could be indeed predicted using either some direct mechanical monitoring of respiration or a real-time estimation of the respiration rate derived from the water frequency NMR monitoring over the previous respiratory cycles. In the first implementation of the field-frequency lock presented in this study, our immediate concern was to avoid the artifactual amplification of the short-term oscillations of the water frequency. For the typical in vivo brain metabolite linewidth currently achieved at 3 T (about 6 Hz in a 15 ml voxel), this deleterious effect would indeed affect the quality of spectroscopic data. A radical way of smoothing any short-term instability of the reference frequency monitored for the field-frequency lock (to avoid the propagation of instabilities onto Z0 correction) would be to average the reference frequency measurements on a longer time scale (from tens to hundreds of seconds). Unfortunately, this simple solution would make the field-frequency lock too sluggish to correct field drift occurring over shorter time periods (a few tens of seconds), which is precisely the interesting range of times for in vivo difference spectroscopy. By performing numerical simulations and realistic phantom experiments, the propagation of the time-correlated frequency fluctuations (related to breathing) onto the Z0 correction was analyzed in detail. The optimum parameters determined for using the field-frequency lock in vivo provided a negligible degradation of the short-term stability of the frequency, while keeping a shorter time window (12 sec) for the averaging of the reference frequency.

The most evident benefit of using a field-frequency lock for in vivo brain MRS is the improvement in linewidth, as shown in this study. Due to the very narrow resonances obtained, even on larger voxels, by adjusting high order shims with analytical methods (7,8), a field drift by a few
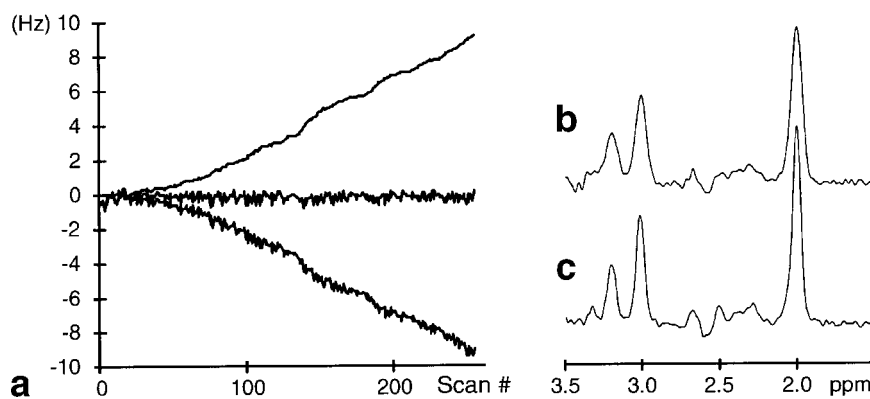
FIG. 6. In vivo data collected on a human head with the interleaved PRESS/pulse-acquire sequence (TR 2 sec, 256 scans) in the presence of a rapid drift of the magnet (about 1 Hz/min) and while the subject was breathing normally (without use of an auditory cue). **a:** The measured reference frequency is plotted for each scan (middle trace), as well as the applied Z0 correction (top trace) and the calculated spontaneous frequency in the absence of correction (bottom trace). **b:** In vivo spectrum from the occipital lobe (15 ml, TE 68 msec) obtained without field-frequency lock for a spontaneous field drift similar to that recorded in **a**. **c:** In vivo spectrum from the occipital lobe (15 ml, TE 68 msec) obtained with field-frequency lock and corresponding to the frequency plots in **a**. Both spectra were processed with a 1 Hz lorentzian broadening.

Hertz during the accumulation of a localized spectrum may affect the observed linewidth. However, this effect becomes truly significant only for a cumulated field shift approaching the intrinsic linewidth of the considered resonance (although not fully intuitive, one can easily show that a lorentzian resonance with a linewidth of 6 Hz will be broadened by only 0.6 Hz for a linear field drift of 3 Hz during the spectrum accumulation, but already by 1.9 Hz for a drift of 6 Hz). Such large field drifts are unusual over the time periods (a few minutes) necessary to accumulate standard single voxel proton spectra, unless the magnet exhibits some atypical behavior at the level of the superconducting coil or of the passive iron shims.

Besides these unfavorable cases, the benefit of the field-frequency lock is also obvious for longer data accumulations (several tens of minutes), as for CSI (9,10) or 2D (11,12) experiments. On the time scale of a 30-min CSI acquisition, even a slow field drift of 0.1 ppm/hr will induce a cumulated frequency shift approaching the typical metabolite linewidth. For such multi-part acquisitions, a simple method is to correct for the field variation by applying a post-processing frequency shift to each individual data set. In this option, the frequency-shift correction factor can be obtained assuming a linear field drift of the magnet. However, this simple solution does not correct for the pejorative effects of the frequency shift on the efficiency of selective pulses used for water suppression or spectral editing (13). In addition, this method does not apply to situations of non-linear field drift, related to an external perturbation or to the heating of the magnet passive iron shims.

A less evident, but certainly significant, benefit of using a field-frequency lock in vivo is expected for localization or editing sequences based on difference spectra, because very strong subtraction artifacts can result from minor frequency shifts (one can easily show that subtracting a lorentzian line with a linewidth of 6 Hz from itself, after a shift by 0.1 Hz, gives a dispersive residual whose peak-to-peak amplitude is about 4% of the original peak). A particularly illustrative case is the combination of an ISIS localization (14) with an editing technique using difference spectroscopy (4,5,15,16). If a full 3D-ISIS localization is performed for each individual spectrum before subtraction, the time interval between the mid-points of the two spectra is typically 20–30 sec. On this time scale the frequency shift due to a normal drift of the magnet is typically 0.1 Hz. Even if such a drift could be corrected in post-processing, provided individual spectra were stored and exhibited a high enough SNR, it seems much more reliable to handle this systematic phenomenon in real time, as demonstrated in this study.

The concept of real-time processing of a reference NMR signal to correct prospectively a source of artifact has already been applied in the field of MRI using navigator echoes (17), especially to reduce motion artifacts during thoracic imaging (18) and brain fMRI (19). A few groups have recently demonstrated that the quality of liver or brain proton NMR spectra can be greatly improved by retrospective navigation (20) or cardiac retro-gating (21), two post-processing approaches that make a close to optimal use of data acquisition time and do not introduce the problematic variability of TR encountered with classical cardiac or respiratory gating. The present study was focused on the real-time correction of the magnet field drift, but it also demonstrates the feasibility of real-time processing on the spectrometer computer to correct various sources of artifacts affecting in vivo NMR spectra.

REFERENCES

1. Gruetter R, Weisdorf SA, Rajanayagan V, Terpstra M, Merkle H, Truwit CL, Garwood M, Nyberg SL, Ugurbil K. Resolution improvements in in vivo ¹H NMR spectra with increased magnetic field strength. J Magn Reson 1998;135:260–264.
2. Gruetter R, Novotny EJ, Boulware SD, Rothman DL, Shulman RG. ¹H NMR studies of glucose transport in the human brain. J Cereb Blood Flow Metab 1996;16:427–438.
3. Gruetter R, Ugurbil K, Seaquist ER. Steady-state cerebral glucose concentrations and transport in the human brain. J Neurochem 1998;70:397–408.
4. Rothman DL, Petroff OAC, Behar KL, Mattson RH. Localized ¹H NMR measurement of γ-aminobutyric acid in human brain in vivo. Proc Natl Acad Sci USA 1993;90:5662–5666.

5. Hetherington HP, Newcomer BR, Pan JW. Measurements of human cerebral GABA at 4.1 T using numerically optimized editing pulses. Magn Reson Med 1998;39:6–10.

6. Bottomley PA. Spatial localization in NMR spectroscopy in vivo. Ann NY Acad Sci 1987;508:333–348.

7. Gruetter R. Automatic, localized *in vivo* adjustment of all first-order and second-order shim coils. Magn Reson Med 1993;29:804–811.

8. Shen J, Rycyna RE, Rothman DL. Improvement of an in vivo automatic shimming method (FASTERMAP). Magn Reson Med 1997;38:834–839.

9. Brown TR, Kincaid BM, Ugurbil K. NMR chemical shift imaging in the three dimensions. Proc Natl Acad Sci USA 1982;79:3523–3526.

10. Pan JW, Twieg DB, Hetherington HP. Quantitative spectroscopic imaging of the human brain. Magn Reson Med 1998;40:363–369.

11. Peres M, Fedeli O, Barrère B, Gillet B, Berenger G, Seylaz J, Beloeil JC. In vivo identification and monitoring of changes in rat brain glucose by two-dimensional shift-correlated ^{1}H NMR spectroscopy. Magn Reson Med 1992;27:356–361.

12. Ziegler A, Metzler A, Köckengerger W, Izquierdo M, Komor E, Haase A, Décorps M, von Kienlin M. Correlation-peak imaging. J Magn Reson B 1996;112:141–150.

13. Shen J, Shungu DC, Rothman DL. In vivo chemical shift imaging of γ-aminobutyric acid in the human brain. Magn Reson Med 1999;41:35–42.

14. Ordidge RJ, Connelly A, Lohman JAB. Image-selected in vivo spectroscopy (ISIS). A new technique for spatially selective NMR spectroscopy. J Magn Reson 1986;66y:283–294.

15. Rothman DL, Novotny EJ, Shulman GI, Howseman AM, Petroff OAC, Mason G, Nixon T, Hanstock CC, Prichard JW, Shulman RG. ^{1}H-[^{13}C] NMR measurements of [4-^{13}C]glutamate turnover in human brain. Proc Natl Acad Sci USA 1992;89:9603–9606.

16. Pan JW, Mason GF, Vaughan JT, Chu WJ, Zhang Y, Hetherington HP. ^{13}C editing of glutamate in human brain using J-refocused coherence transfer spectroscopy at 4.1 T. Magn Reson Med 1997;37:355–358.

17. Ehman RL, Felmlee JP. Adaptive technique for high-definition MR imaging of moving structures. Radiology 1989;173:255–263.

18. Sachs TS, Meyer CH, Hu BS, Kohli J, Nishimura DG, Makovski A. Real-time motion detection in spiral MRI using navigators. Magn Reson Med 1994;32:639–645.

19. Lee CC, Jack CR Jr, Grimm RC, Rossman PJ, Felmlee JP, Ehman RL, Riederer SJ. Real-time adaptative motion correction in functional MRI. Magn Reson Med 1996;36:436–444.

20. Tyszka JM, Silverman JM. Navigated single-voxel proton spectroscopy of the human liver. Magn Reson Med 1998;39:1–5.

21. Felblinger J, Kreis R, Boesch C. Effects of physiologic motion of the human brain upon quantitative ^{1}H-MRS: analysis and correction by retro-gating. NMR Biomed 1998;11:107–114.